How to Cite:
Lateef, N. T., & Al-Fahdawi, A. S. (2022). Synthesis of nano-oxides by preparing metal complexes based on dithiocarbamate derivatives. *International Journal of Health Sciences*, *6*(S4), 10460–10470. https://doi.org/10.53730/ijhs.v6nS4.12213

Synthesis of nano-oxides by preparing metal complexes based on dithiocarbamate derivatives

Nisreen Talib Lateef
Department of Chemistry, College of Education for Pure Sciences, University of Anbar, Iraq
Corresponding author email: nis13u4016@uoanbar.edu.iq

Aeed Salih Al-Fahdawi
Department of Chemistry, College of Education for Women, University of Anbar, Iraq Ramadi
Email: edw.aeedchemistry@uoanbar.edu.iq

***Abstract*---**Metal oxide nanoparticles are a branch of nanoparticles that have high optical properties. Dithiocarbamites are organic sulfur bonds that form stable complexes with metals. There are two types of dithiocarbamate: mono- and di-alkyl dithiocarbamate. In this study, two Schiff bases were prepared, the first Schiff base: [(E)-N-(2-ethylhexyl)-1-Phenyl methanimine] and the second Schiff base: [(E)-N-benzyl-1-Phenyl methanimine]. From these two bases, the first secondary amine was prepared: N-Benzyl-2-ethylhexyl-1-amine, and the second secondary amine, Di Benzylamine. This was followed by the preparation of ligands from the two prepared secondary amines, which are Potasium benzyl(2-ethyl) Carbamadithioate, and the second ligand: Potasium di benzyl Carbamodithioate. These two ligands were employed in the interaction with the ions: Mn, Cu, Zn. each separately to form the macrocyclic complexes. The characterized methods showed the success of the preparing method of nano-oxides through several prominent results, such as: the electronic transitions of the group S-C=S, N-C=S and sulfur atoms, the disappearance of the absorption band at (3360) cm-1, which belongs to the (NH2 ν) bond at the base Schiff compared to the primary amine, chemical shift from 7.33 ppm to 7.98 ppm (5H) is due to the aromatic ring protons, chemical shift from δ=128.86 ppm to δ=130.71 ppm (5C) is due to the aromatic ring carbons (C1-C2-C3-,C4-C5). SEM analysis of the Mn(L1) complex appeared as small crystal segments with size ranging between (18.12-23.37nm), The zinc complex Zn(L1) is large crystals resembling small polygonal spheres and cylinders with a size of (268.30nm).

International Journal of Health Sciences ISSN 2550-6978 E-ISSN 2550-696X © 2022.
Manuscript submitted: 9 April 2022, Manuscript revised: 18 June 2022, Accepted for publication: 27 July 2022

***Keywords*---**nano-oxides, metal complexes, dithiocarbamate.

Introduction

Greek word "nano" means "dwarf" or "abnormally little item." It is used as a prefix to a unit, such the second or the meter [(1)]. According to the United States Environmental Protection Agency, nanotechnology is the study and manipulation of materials with dimensions of around 1-100 nanometers, where special physical features enable the development of novel applications [(2)]. One must be aware that a single human hair is 60,000 nanometers thick and that the DNA double helix has a radius of 1 nanometer as a point of comparison [(3)]. Information technology, energy, environmental sciences, medical, homeland security, food safety, and transportation are just a few of the technological and industrial industries that nanotechnology is significantly advancing and revolutionizing. The latest developments in chemistry, physics, materials science, and biology are combined with nanotechnology to produce novel materials with special qualities because their structures are specified on the nanoscale size. This essay lists the different ways that nanotechnology has been used in recent years [(4)]. Dithiocarbamates (dtcs) are stable complexes of organic sulfur bonds with metals [(5)]. Dithiocarbamate comes in two varieties: mono- and di-alkyl dithiocarbamate. Depending on the type of amines utilized during the compound's synthesis, the two are synthesized. Early in the 20th century, precisely around the year 1930, is when the chemistry of dicarbomet first emerged. The first time a fungicide was employed commercially was during World War II. Additional widespread uses include quickening the vulcanization process, serving as flotation agents, functioning as pesticides in agriculture, biology, materials science, medicine, organic synthesis, light-stabilizing polymers, and radiator protection [(6)]. The methods used to characterize dithiocarbamate and the coordination compounds are quite similar. Solubility tests, physical and chemical characteristics (such as melting point and molar conductivity (MC)), elemental analysis, spectroscopy (UV, infrared, photoluminescence), magnetic moment, and microwave spectroscopy are examples of characterization procedures (NMR, echomagnetic electron). There is a need for more characterisation methods for nanoparticles and nanocomposites. such as energy dispersive X-ray spectroscopy (EDX/EDS), thermal analysis, scanning electron microscopy (SEM), transmission electron microscopy (TEM), and X-ray diffraction (XRD) (TA).

Materials and Methods

Preparation of Schiff base 1 (E)-N-(2-ethylhexyl)-1-Phenyl methanimine

Synthesis of Schiff bases 20 mL of methanol, 1 (E)-N-(2-ethylhexyl)-1-phenyl methanimine, and 3–4 drops of HBr were continuously stirred into 1.2 mL of benzoledehyde. The mixture was heated, adding 0.8 ml of 2-Ethyle-hexylamine progressively dissolved in 20 ml of methanol, and allowed to continue heating for the duration of the thermal escalation process (3 hours). In order to produce a white precipitate, the mixture was cooled and the solvent evaporated at ferophilic pressure. The white precipitate was then filtered and weighed (2.007 g) at a percentage of (98%) [(7)].

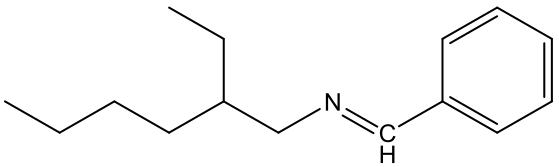

(*E*)-*N*-(2-ethylhexyl)-1-phenylmethanimine

Figure (1): Schiff base 1

Preparation of the secondary amine 1 N-Benzyl-2-ethylhexyl-1-amine

Schiff's secondary amine 1, N-benzyl-2-ethylhexyl-1-amine, was synthesized. It weighs 0.5 g. 20 ml of methanol containing 1 base was added to an ice bath while being constantly stirred, and 0.17 g of NaBH4 was progressively added while being stirred for (12 hours). Distilled water was added to the Di Chloromethane solution to separate the organic layer. The organic layer was then washed three times with water at a ratio of (3 x 50 ml). MgSO4 was used to dry it, and after the solution was filtered and evaporated under vacuum pressure, a yellow-colored oily material with a proportion of (67.40%) was the result [8].

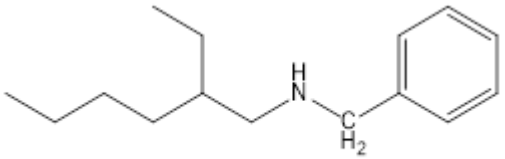

N-benzyl-2-ethylhexan-1-amine

Figure (2): Secondary Amine 1

Preparation of the ligand 1 Potasium benzyl(2-ethyl) Carbamadithioate

Ligand 1's synthesis uses potassium benzyl (2-ethyl) With constant stirring for 30 minutes, 0.11 g of KOH was dissolved in 3 ml of ethanol, and 0.23 g of the previously synthesized secondary amine 1 was dissolved in carbamadithioate (15 minutes). After cooling the mixture in an ice bath, 0.22 ml of CS2 was added, and the mixture was allowed to stir constantly for two hours to produce the precipitate, dithiocarbamate salt, which had been filtered and cleaned with methanol and ether. Then, it was dried under vacuum pressure to produce the white precipitate shown in the diagram, which was produced by weight (0.32 g) and by (95.2%). Figure (3).

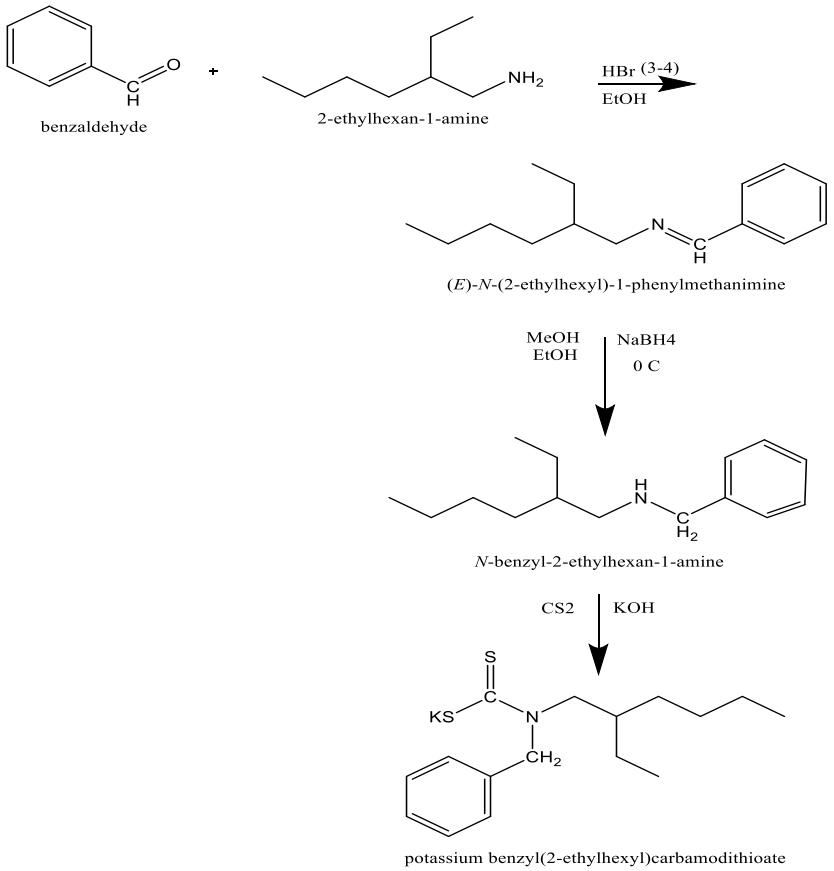

Figure (3): Potasium benzyl(2-ethyl) Carbamadithioate

Large Ring Complex Preparation

As the metals used to prepare the cyclic complexes are (Mn, Fe, Co, Ni, Cu, Zn), the complexes were made by reacting one mole of potassium dithiocarbamate salt (KDTC) representing as a ligand against one mole of metal salt representing as the central ion to get the ratio (1:1). The mixture of the ligand salt, metal, and its solvents was stirred for three hours, and distilled water was added In order to create the cyclic complex, the precipitate was collected by filtering, washed with solvent, and dried to produce complexes of various colors.

Synthesis of [Cu(L1)]2 Complex

Producing [Cu(L1)] 2 The complex (0.32 g) of potassium dithiocarbamate salt 1 (KDTC 1) was dissolved in 30 ml of ethanol, and the solution was progressively supplemented with (0.19 g) of CuCl2.2H2O while being constantly stirred. Immediately after combining, the color changed, and it was left to continually swirl for (3 hours). The precipitation will thereafter be a deep green color. To eliminate the unreacted organic debris, the precipitate was filtered and washed with a tiny amount of ethanol and diethyl ether. It was then dried under vacuum pressure to produce a product with a weight of 0.48 g and a percentage of 78.6%.

Synthesis of [Mn(L1)]2 Complex

Potassium dithiocarbamate 1 salt (0.32 g) was dissolved in 30 ml of ethanol, and then MnCl2.4H2O (0.19 g) was dissolved in 30 ml of ethanol and added gradually while being constantly stirred. When the mixture's color changed at the time of mixing and was constantly stirred for three hours, a brown precipitate eventually developed. To eliminate the unreacted organic matter, the precipitate was filtered and washed with a tiny amount of ethanol and diethyl ether. It was then dried under vacuum pressure to produce a product with a weight of 0.42 g and a percentage of (70%).

Preparation of Nanoparticles from Complexes

Preparation of CuO NPs

Thermal analysis was needed to produce CuO Nps from 1 g of Cu(L)2 complexes. CuO nanoparticles eventually formed after the copper complex was heated to 400°C in an incineration furnace and placed in a ceramic bowl (3 hours). AFM, SEM, and XRD were used to characterize the resultant CuO Nps after the final product had been washed with ethanol more than three times to reduce impurities and dried at (25°C) for three days.

Preparation of MnO NPs

(1 g) of Mn(L)2 complexes was utilized to produce MnO Nps by thermal analysis. At a temperature of (400°C), the manganese complex was placed in a ceramic bowl in the incineration furnace, and eventually the MnO nanoparticles were created (3 hours). AFM, SEM, and XRD were used to diagnose the resultant MnO Nps after the final product had been washed with ethanol more than three times to eliminate impurities and dried at temperature (25°C) for three days.

Results and Discussions

FTIR spectra of complexes

The absorption bands between 611-450 cm-1, (1120-811) cm-1, and (1440-1497) cm-1 are the basis for the regions of interest in the FTIR spectra of metal complexes. Since the bands at frequency (611) 450 cm-1 are part of the v(M-S) band, the bands between frequencies (1120 and 811) cm-1 are part of the (C-S), and the third region is at (1440- 1479) cm-1 is related to the (C-N) band of the (NCS2) band. Due to the poles of the group's form (+N = CS2, the presence of the band in the region (1479) cm-1 is anticipated. Along with raising the wavenumber of the (C-N) bond, boosting the electronegative nature of the alkyl group will contribute in the stability of this structure.

Figure (4) shows the FTIR spectra of the first ligand and its complexes. The strong band in the complexes' spectra in the region of (1408-1497) cm-1 is ascribed to the stretching of the v(N-CS2) bond. The frequencies of this bond were compared to the ligand's identical bond's absorption band at (1497) cm^{-1}. Regarding the ligand's absorption band at frequency (955) cm-1, it relates to the band stretch vs

(CS2). New absorption bands that are related to the M-S bond in the complexes of the first ligand include the Mn-S 608 cm-1, Cu-S 699 cm^{-1}.

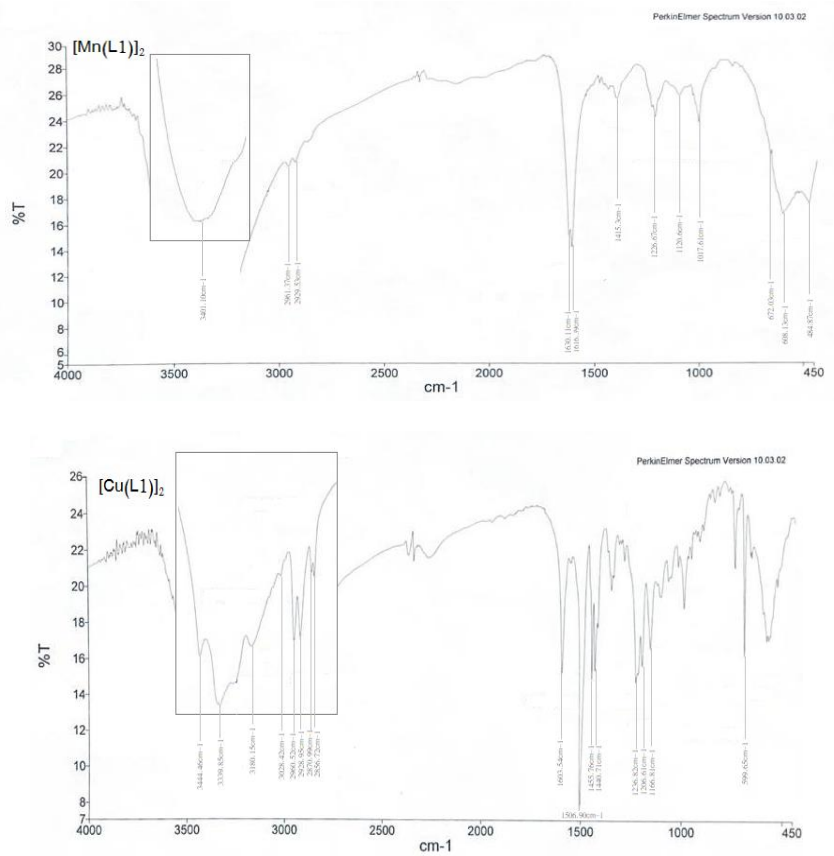

Figure (4): FTIR spectra of complexes

^{1}H-NMR spectrum of the zinc complex (1)

The signal at the chemical displacement =0.77-0.87 ppm (12H) owing to (C14,14,16,16-H) is attributable to (CH3) protons, as seen in the 1H-NMR spectrum of zinc complex (1) in Figure 5. The apparent signal at the chemical displacement between 2.61 and 2.63 ppm (16H) is caused by (C11,11,12,12,13,13,15,15 -H) protons. The protons are responsible for the signal seen at a chemical displacement of =3.85 ppm (2H) (SH). The imine protons (C7,7,9,9-H) are to responsible for the chemical displacement at = 5.30–5.38 ppm (8H) (H-C-N). The signal at the chemical displacement between 1.14 and 1.57 ppm (2H) is caused by the protons (C10,10-H) (CH). While the aromatic ring protons are responsible for the chemical displacement from 7.27 ppm to 7.49 ppm (10H). The remaining water is what causes the sign at chemical displacement =3.38 ppm, and the protons from the solvent DMSO-d6 are what causes the apparent sign at chemical displacement =2.50-2.52 ppm.

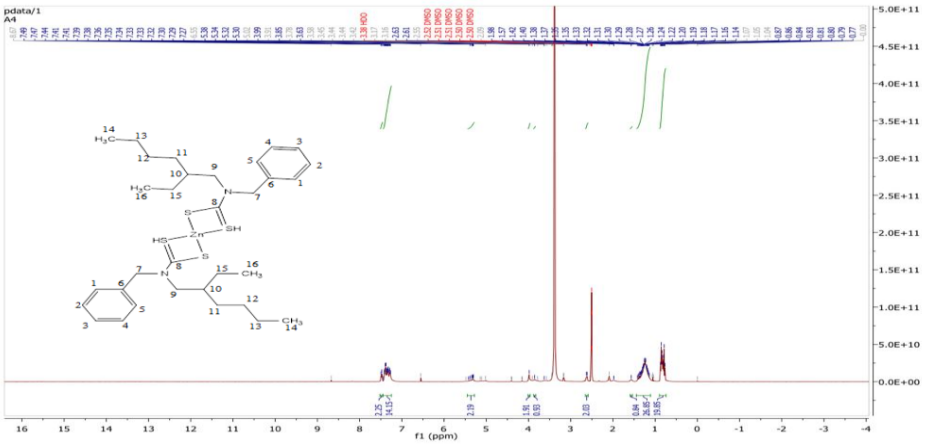

Figure (5): ^{1}H-NMR spectrum of zinc complex (1).

^{13}C-NMR spectrum of the zinc complex (1)

Figure 5 of the zinc complex (1)'s 13C-NMR spectrum illustrates the chemical displacement caused by an atom at ppm = 22.88-28.46 (8C) (C11,11,12,12,13,13,15,15). It's part of a group (CH2). The group (CH3) is responsible for the chemical displacement at ppm =10.77-14.45 (4C), whereas an atom (C14,14,16,16) is responsible for the displacement at ppm =39.39-39.61 (2C) (C10, 10) The (CH) group is responsible for this displacement, while the solvent residue DMSO-d6 is responsible for the sign at chemical displacement =39.72-40.56 ppm (2). The absence of chemical displacement from the NCS2 group (C8,8). Additionally, it was not revealed how the carbon atoms in the aromatic ring were moved chemically.

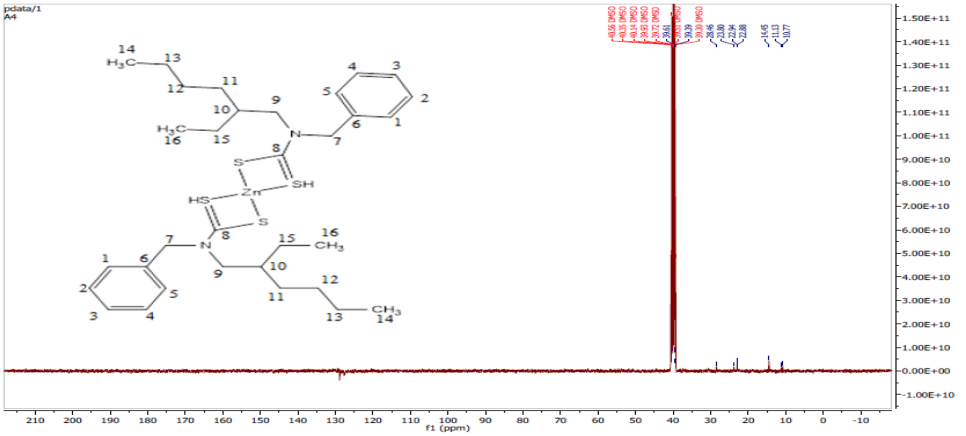

Figure (6): 13C-NMR spectrum of zinc complex (1)

Scanning electron microscopy analysis of Mn(L1) manganese complex

SEM analysis of the Mn(L1) complex appeared as small crystal segments with size ranging between (18.12-23.37nm) as shown in Figure (7).

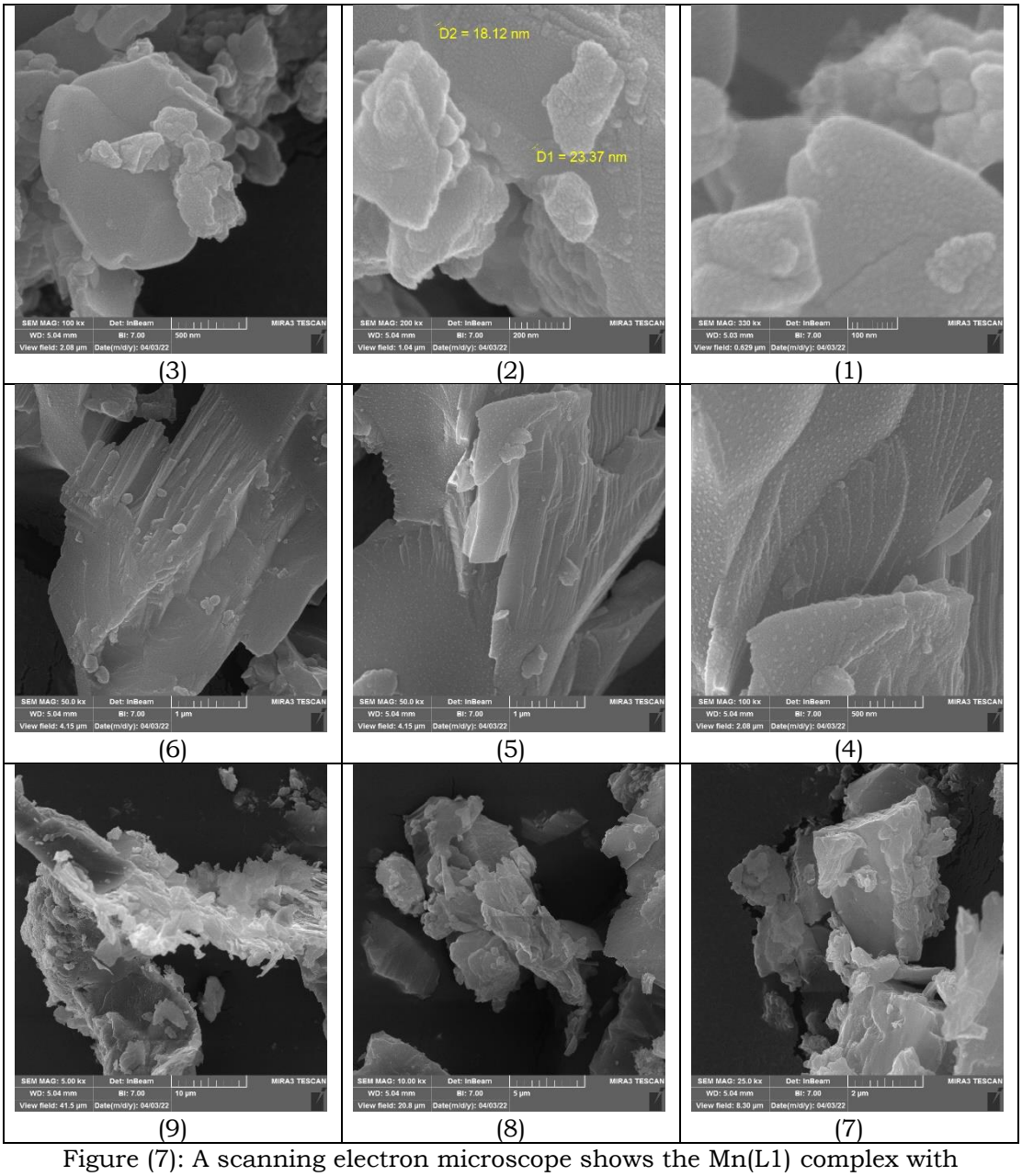

Figure (7): A scanning electron microscope shows the Mn(L1) complex with different magnifications of the images

X-ray diffraction analysis of Mn(L1) manganese complex

The X-ray diffraction spectrum of the Mn(L1) complex in Fig. (8) showed fourteen reflections and the highest intensity was at 2θ = 31.444 corresponding to the value of XS = 22nm. It was found that the Mn(L1) complex possesses an octahedral system. Table (1) shows the X-ray diffraction data for the Mn(L1) manganese complex.

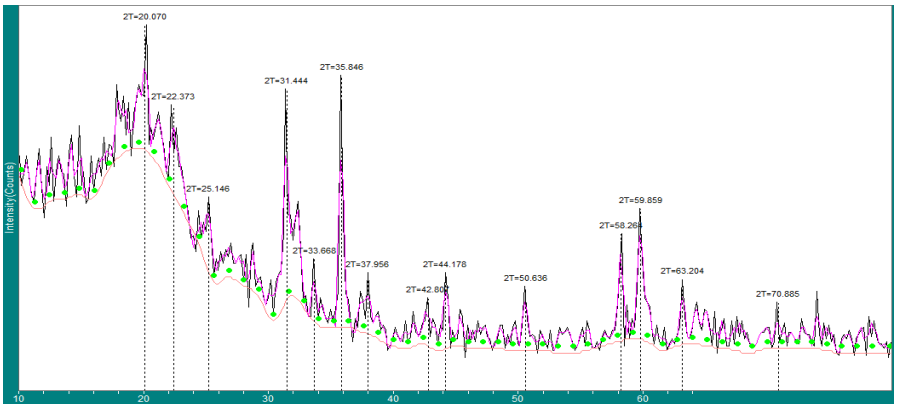

Figure (8): X-ray diffraction spectrum of Mn(L1) manganese complex.

Table (1): X-ray diffraction data for Mn(L1) complex

Peak	2-Theta	d(nm)	BG	Height	I%	Area	I%	FWHM	Crystal Size XS (nm)
1	20.07	0.44205	104	55	50	169	44	0.522	15
2	22.373	0.39704	87	37	33.6	144	37.5	0.662	12
3	25.146	0.35386	51	33	30	97	25.3	0.5	16
4	31.444	0.28427	38	93	84.5	384	100	0.702	11
5	33.668	0.26598	30	27	24.5	62	16.1	0.39	22
6	35.846	0.2503	27	110	100	217	56.5	0.335	26
7	37.956	0.23686	24	27	24.5	107	27.9	0.674	12
8	42.807	0.21107	19	21	19.1	80	20.8	0.648	13
9	44.178	0.20483	18	33	30	76	19.8	0.392	22
10	50.636	0.18012	17	28	25.5	73	19	0.443	20
11	58.264	0.15823	21	47	42.7	108	28.1	0.391	24
12	59.859	0.15438	22	57	51.8	198	51.6	0.591	15
13	63.204	0.147	20	28	25.5	65	16.9	0.395	24
14	70.885	0.13283	18	20	18.2	45	11.7	0.383	26

X-ray diffraction analysis of the zinc complex Zn(L1)

The X-ray diffraction spectrum of the zinc complex Zn(L1) in Figure (9) showed fourteen reflections and the highest intensity was at 2θ = 54.547 corresponding to the value of XS = 26nm, and it was found that the zinc complex Zn(L1) possesses a tetrahedral system. Table (2) shows the X-ray diffraction data for the Zn(L1) zinc complex.

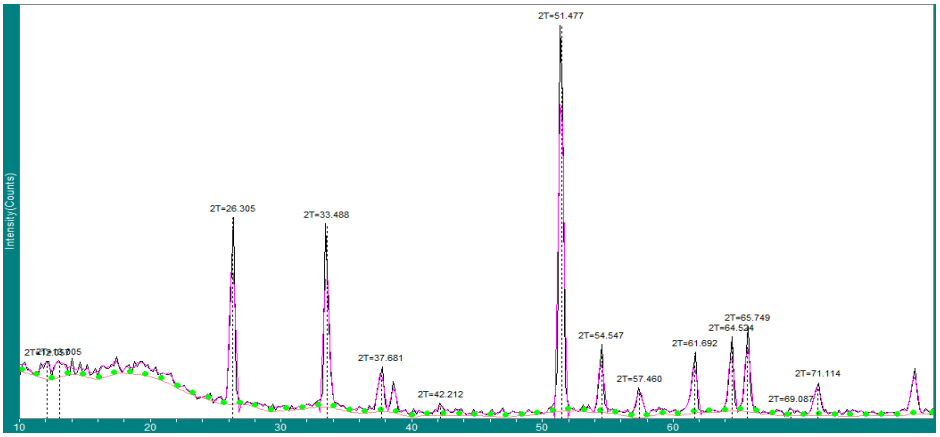

Figure 9: X-ray diffraction spectrum of Zn(L1) zinc complex

Table (2): X-ray diffraction data for Zn(L1) zinc complex.

Peak	2-Theta	d(nm)	BG	Height	I%	Area	I%	FWHM	XS(nm)
1	12.057	0.73347	72	35	4.8	123	8	0.597	13
2	13.005	0.6802	75	33	4.5	154	10.1	0.793	10
3	26.305	0.33852	25	355	48.4	710	46.4	0.34	25
4	33.488	0.26737	20	348	47.4	733	47.9	0.358	24
5	37.681	0.23853	11	85	11.6	290	18.9	0.58	14
6	42.212	0.21391	4	23	3.1	88	5.7	0.65	13
7	51.477	0.17738	11	734	100	1531	100	0.355	25
8	54.547	0.1681	9	130	17.7	274	17.9	0.358	26
9	57.46	0.16025	0	57	7.8	167	10.9	0.498	18
10	61.692	0.15023	8	116	15.8	296	19.3	0.434	21
11	64.524	0.1443	12	141	19.2	274	17.9	0.33	29
12	65.749	0.14191	11	162	22.1	337	22	0.354	27
13	69.087	0.13584	3	15	2	60	3.9	0.68	14
14	71.114	0.13246	4	62	8.4	192	12.5	0.526	18

Conclusion

The atomic force microscopy images of the prepared nanoparticles (CuO Nps, MnO Nps, and ZnO Nps) revealed that they are nearly identical in terms of size, with a diameter ranging from between 40 and 80 nanometers. The scanning electron microscope images of the prepared nanoparticles (CuO Nps, MnO Nps, and ZnO Nps) demonstrated the homogeneity of their surfaces with a diameter ranging from 25 to 80 nm.

References

Baig, N., Kammakakam, I., & Falath, W. (2021). Nanomaterials: a review of synthesis methods, properties, recent progress, and challenges. Materials Advances, 2(6), 1821–1871. https://doi.org/10.1039/D0MA00807A

Bayda, S., Adeel, M., Tuccinardi, T., Cordani, M., & Rizzolio, F. (2019). The History of Nanoscience and Nanotechnology: From Chemical–Physical Applications to Nanomedicine. Molecules, 25(1), 112. https://doi.org/10.3390/molecules25010112.

Boholm, M. (2016). The use and meaning of nano in American English: Towards a systematic description. Ampersand, 3, 163–173. https://doi.org/10.1016/j.amper.2016.10.001

Cele, T. (2020). Preparation of Nanoparticles. In Engineered Nanomaterials - Health and Safety. IntechOpen. https://doi.org/10.5772/intechopen.90771

Kouhi, A. (2018). Integrating Nanotechnology Into Engineered Products. In Reference Module in Biomedical Sciences. Elsevier. https://doi.org/10.1016/B978-0-12-801238-3.65571-X.

Mukhopadhyay, S., Parshad, V. R., & Gill, I. (2009). Nanoscience and Nano-Technology: Cracking Prodigal Farming. Nature Precedings. https://doi.org/10.1038/npre.2009.3203.

Santos, P. M., Simões, T., and Sá-Correia, I1 (2449)1 Insights into yeast adaptive response to the agricultural fungicide mancozeb: a toxicoproteomics approach. Proteomics, 9(3), 657- 670.

Susilo, C. B., Jayanto, I., & Kusumawaty, I. (2021). Understanding digital technology trends in healthcare and preventive strategy. *International Journal of Health & Medical Sciences*, *4*(3), 347-354. https://doi.org/10.31295/ijhms.v4n3.1769

Takii, T., Onozaki, K., Mori, M., Kuroishi, R., Ito, S., Chiba, T., ... and Horita, Y. (2012). The potential therapeutic usage of dithiocarbamate sugar derivatives for multi-drug resistant tuberculosis. INTECH Open Access Publisher.

Widana, I.K., Sumetri, N.W., Sutapa, I.K., Suryasa, W. (2021). Anthropometric measures for better cardiovascular and musculoskeletal health. *Computer Applications in Engineering Education*, *29*(3), 550–561. https://doi.org/10.1002/cae.22202